3402 *Inorg. Chem.* **2010**, *49*, 3402–3408
DOI: 10.1021/ic902514w

Inorganic Chemistry
Article

Structural Study of Mixed Crystals of $[Zn_{1-x}Ru_x(bpy)_3][NaCr(ox)_3]$ Probed by High-Resolution Absorption Spectroscopy and High-Pressure Experiments

Mia Milos, Tiphaine Penhouet, Prodipta Pal, and Andreas Hauser*

Université de Genève, Département de Chimie Physique, 30 quai Ernest-Ansermet, CH-1211 Genève 4, Switzerland

Received December 17, 2009

In the mixed crystal series of the cubic three-dimensional networks of composition $[Zn_{1-x}Ru_x(bpy)_3][NaCr(ox)_3]$ ($0 \leq x \leq 1$, ox = $C_2O_4^{2-}$, bpy = 2,2′-bipyridine), high-resolution absorption spectroscopy in the region of the $^4A_2 \rightarrow {}^2E$ transition (R-lines) reveals the creation of five specific spectroscopic sites for the $[Cr(ox)_3]^{3-}$ complex. The concentration of these spectroscopic sites follows a binomial distribution of $[Zn(bpy)_3]^{2+}$ and $[Ru(bpy)_3]^{2+}$ among the four nearest neighbors of a given $[Cr(ox)_3]^{3-}$ complex within the network. The tris-bipyridine complexes occupying those positions have an optimal $\pi-\pi$ interaction with the oxalate ligands of the tris-oxalate chromophore. The energy of each spectroscopic $[Cr(ox)_3]^{3-}$ site depends on the total concentration of $[Ru(bpy)_3]^{2+}$ in the mixed crystal and on its specific distribution among the four nearest neighbors. Single crystal X-ray diffraction indicates a reduction of the unit cell volume when $[Zn(bpy)_3]^{2+}$ (a = 15.6365(18) Å) is substituted by $[Ru(bpy)_3]^{2+}$ (a = 15.5098(6) Å). This alone would lead to a red-shift of the R lines in analogy to the red-shift of 25.2 cm^{-1}/GPa due to the decrease of the metal ligand Cr−O bond length as observed in high-pressure luminescence experiments. However, specific $\pi-\pi$ interactions with the nearest neighbors have the opposite effect and shift the transition in discrete jumps to higher energies with increasing $[Ru(bpy)_3]^{2+}$ mole fraction.

1. Introduction

Three dimensional oxalate networks of general composition $[M^{II}(bpy)_3][M^IM^{III}(ox)_3]$, $[M'^{III}(bpy)_3][M^{II}M^{III}(ox)_3]$, and $[M'^{III}(bpy)_3][M^IM^{III}(ox)_3]ClO_4$ (ox = $C_2O_4^{2-}$; bpy = 2,2′-bipyridine; M^I = Li, Na; M^{II} = Ru, Zn, Co, Fe, Mn, etc.; M^{III} = Al, Cr, Rh, etc.; M'^{III} = Rh, Cr) were first synthesized by Decurtins et al.[1,2] In this class of compounds, the tris-bipyridine cation tightly fits into the cavities provided by the three-dimensional polymeric anionic $[M^IM^{III}(ox)_3]_\infty$ network. They are of interest because of their magnetic properties,[3] such as ferro- and antiferromagnetic order[4] or the incorporation of a spin-crossover function.[5] Likewise, they possess unique photophysical properties as exemplified by several energy transfer studies with the $[Cr(ox)_3]^{3-}$ complex as the active chromophore.[6] The lowest excited state of $[Cr(ox)_3]^{3-}$ is the ^2E state, and it is spectroscopically accessible via the spin-forbidden $^4A_2 \rightarrow {}^2E$ spin-flip transition in the form of a sharp doublet (R-lines) due to the zero-field splitting of the ^2E state. This feature makes the $[Cr(ox)_3]^{3-}$ complex a very interesting chromophore, since small variations in the local geometry around the chromophore affect absorption as well as luminescence spectra. For instance, in mixed crystals of composition $[Rh(bpy)_3][NaAl_xCr_{1-x}(ox)_3]ClO_4$, increasing the Cr^{3+} concentration leads to a decrease of the inhomogeneous broadening of the R lines from initially 5.9 cm^{-1} at $x < 0.1$ to 3.8 cm^{-1} at $x > 0.9$ and is accompanied by a shift to higher energy of 1.7 cm^{-1}.[6]

In this article, we present a series of mixed crystals of composition $[Zn_{1-x}Ru_x(bpy)_3][NaCr(ox)_3]$, where the mole fraction of the $[Cr(ox)_3]^{3-}$ chromophore is kept at 100%, and we investigate the influence of the complexes sitting in the cavity of the oxalate network on the $^4A_2 \rightarrow {}^2E$ transition as a function of the $[Ru(bpy)_3]^{2+}$ mole fraction. We will show that rather than just create disorder resulting in nonspecific inhomogeneous broadening of the R-lines, we create specific spectroscopic sites for $[Cr(ox)_3]^{3-}$, which manifest themselves in additional splittings and concentration dependent shifts. In order to fully understand the different effects, we also investigate the shift of the R-lines as a function of external pressure. Finally, we propose a model which, for a given mole fraction of $[Ru(bpy)_3]^{2+}$, gives the population distribution and energy of each individual specific site.

*To whom correspondence should be addressed. E-mail: Andreas.Hauser@unige.ch.

(1) Decurtins, S.; Schmalle, H. W.; Schneuwly, P.; Ensling, J.; Gütlich, P. *J. Am. Chem. Soc.* **1994**, *116*, 9521.
(2) Decurtins, S.; Schmalle, H. W.; Pellaux, R.; Schneuwly, P.; Hauser, A. *Inorg. Chem.* **1996**, *35*, 1451.
(3) Pointillart, F.; Train, C.; Gruselle, M.; Villain, F.; Schmalle, H. W.; Talbot, D.; Gredin, P.; Decurtins, S.; Verdaguer, M. *Chem. Mater.* **2004**, *16*, 832.
(4) Coronado, E.; Galan-Mascaros, J. R.; Gomez-Garcia, C. J.; Martinez-Ferrero, E.; Almeida, M.; Waerenborgh, J. C. *Eur. J. Inorg. Chem.* **2005**, 2064.
(5) Zerara, M.; Hauser, A. *ChemPhysChem* **2004**, *5*, 395.
(6) von Arx, M. E.; Langford, V. S.; Oetliker, U.; Hauser, A. *J. Phys. Chem. A* **2002**, *106*, 7099.

Published on Web 02/24/2010
© 2010 American Chemical Society

2. Experimental Methods

2.1. Materials. The starting materials, $K_3Cr(ox)_3 \cdot 3H_2O$ and $[Ru(bpy)_3]Cl_2 \cdot 6H_2O$, were synthesized according to literature procedures.[7,8] $[Zn(bpy)_3]Cl_2 \cdot 6H_2O$ was prepared by adding $ZnCl_2$ to 3 equivalents of 2,2′-bipyridine in boiling water followed by slow evaporation of the solvent. The following chemicals were used as received: $RuCl_3 \cdot$hydrate, purum (Fluka); 2,2′-bipyridine, puriss. (Fluka); $ZnCl_2$ anhydrous, purum (Fluka); $K_2(ox) \cdot H_2O$, purum (Fluka); $H_2C_2O_4 \cdot 2H_2O$, ultra (Fluka); $K_2Cr_2O_7$ (Aldrich), NaCl (Aldrich).

2.2. Synthesis of Mixed Crystals of Composition $[Zn_{1-x}Ru_x(bpy)_3][NaCr(ox)_3]$, $0 \le x \le 1$. The neat compounds (x = 0 and 1) were prepared according to the literature method of Decurtins and co-workers.[2] Accordingly, 10^{-2} M aqueous solutions of $K_3Cr(ox)_3$, $[Ru(bpy)_3]Cl_2 \cdot 6H_2O$, $[Zn(bpy)_3]Cl \cdot 6H_2O_2$, and NaCl were prepared. To obtain $[Zn(bpy)_3][NaCr(ox)_3]$ and $[Ru(bpy)_3][NaCr(ox)_3]$, 20 mL of the $K_3Cr(ox)_3$ and NaCl solutions were added to the same volumes of $[Zn(bpy)_3]^{2+}$ or $[Ru(bpy)_3]^{2+}$ solutions, respectively. Single crystals of the neat compounds in the form of perfect tetrahedra of a 0.5 mm edge were obtained by slow evaporation of the solutions stored at 5 °C in a refrigerator.

The series of $[Zn_{1-x}Ru_x(bpy)_3][NaCr(ox)_3]$ mixed crystals was obtained by adding different volumes of the $[Zn(bpy)_3]^{2+}$ and $[Ru(bpy)_3]^{2+}$ solutions in order to have the nominal values of x = 0, 0.05, 0.1, 0.2, 0.4, 0.6, 0.8, and 1. Crystals were obtained of the mixed compounds in the same way as for the neat compounds. The effective Zn^{2+} and Ru^{2+} concentrations were determined by inductively coupled plasma−mass spectrometry (ICP-MS) and resulted in effective x values of 0, 0.18, 0.31, 0.44, 0.58, 0.76, 0.90, and 1, respectively. Powder samples were prepared by quick precipitation while stirring the mixture. For the same nominal ratios, the ICP-MS analysis gave real x values of 0, 0.23, 0.39, 0.56, 0.78, 0.89, 0.96, and 1, respectively.

2.3. X-Ray Diffraction. A crystal of size 0.2 × 0.1 × 0.04 mm was selected and mounted on a glass fiber. Data were collected on a STOE IPDS II image plate diffractometer using Mo Kα radiation at 293 K. Integration of the data and absorption correction were done in the X-area software.[9] The structure was solved using the charge flipping method in the program Superflip[10] and refined by full matrix least-squares procedures on F^2 using Crystals.[11] H atom positions could be located on Fourier difference maps but were recalculated geometrically. They were refined with strong restraints for a few cycles and then were allowed to ride on their parent atoms during the rest of the refinement. Crystallographic data: formula $C_6CrNaO_{12} \cdot C_{30}H_{24}N_6Ru$, space group $P2_13$, Z = 4, a = 15.5098 (6) Å, 32 468 reflections measured, face-indexed absorption correction Tmin = 0.89, Tmax = 0.97, 3349 independent reflections (Rint = 0.097) of which 2442 with a resolution larger than 0.81 Å were used in the least-squares refinement, 172 parameters, R = 0.0492, wR = 0.0662, S = 0.8736, min and max residual peak density −0.54/0.63 e·Å^{-3}, Flack parameter 0.01(4). X-ray powder diffraction diagrams of mixed $[Zn_{1-x}Ru_x(bpy)_3][NaCr(ox)_3]$, $0 \le x \le 1$, at room temperature were obtained on a Bruker Advanced D8 diffractometer using Bragg−Brentano geometry in the reflection mode, monochromatic Cu $K_{\alpha 1}$ radiation, and a PSD detector. The powder diffraction patterns were fitted by profile matching with the FullProf software[12] within space group $P2_13$, using the initial parameters for neat $[Zn(bpy)_3][NaCr(ox)_3]$ and the lattice constant a as the only free parameter.[13]

2.4. High-Resolution Absorption Spectroscopy. Electronic absorption spectra were obtained on single crystals using a Fourier-transform spectrometer equipped for measuring in the infrared and visible spectral range (Bruker IFS66/S). The absorption spectra were collected at a spectral resolution of 0.5 cm^{-1}. For absorption measurements, crystals with one corner of the tetrahedron polished down to a thickness of ∼60 μm were mounted on copper apertures, placed in a closed cycle cryostat (Oxford Instruments CCC1204), and collected at 10 K in an atmosphere of He exchange gas.

2.5. High-Pressure Luminescence Measurements. Luminescence measurements were performed at 10 K using the same closed cycle cryostat and the FT spectrometer as for the absorption measurements. High pressures were achieved using a diamond anvil cell (MiniDAC of D'Anvils Ltd.). The sample chamber consisted of a hole with a diameter of 400 μm drilled into a preindented metal gasket. A single crystal of neat $[M(bpy)_3][NaCr(ox)_3]$ (M = Zn or Ru) was placed in the sample chamber with a crystal of Sm^{2+}:BaFCl used to calibrate the pressure inside the DAC (note, ruby cannot be used as its R-lines are at exactly the same energy as those of $[Cr(ox)_3]^{3-}$). A 4:1 methanol/ethanol mixture was used as the pressure-transmitting medium. The crystals were excited at 532 and 405 nm (< 10 mW) using laser diodes in order to selectively obtain the luminescence from the $[Cr(ox)_3]^{3-}$ and Sm^{2+} chromophores, respectively. The $^5D_0 \rightarrow {}^7F_0$ transition of Sm^{2+} is centered at 14 531 cm^{-1} and is not split further by spin−orbit coupling. The shift rate of the $^5D_0 \rightarrow {}^7F_0$ transition of Sm^{2+} is −21 cm^{-1}/GPa.[14] The exact position of the $^5D_0 \rightarrow {}^7F_0$ luminescence band was determined with a Gaussian fit, and using the above shift rate, the pressure within the DAC was established for each experiment.

3. Results

3.1. Crystal Structure of $[Zn_{1-x}Ru_x(bpy)_3][NaCr(ox)_3]$, $0 \le x \le 1$. The three-dimensional networks of the neat compounds $[Zn(bpy)_3][NaCr(ox)_3]$ and $[Ru(bpy)_3][NaCr(ox)_3]$ crystallize in the cubic and chiral space group $P2_13$ with Z = 4.[13] The single crystal structure of $[Zn(bpy)_3][NaCr(ox)_3]$ has been reported previously.[13] Details of the single crystal structure determination of $[Ru(bpy)_3][NaCr(ox)_3]$ are given in the Supporting Information. The site symmetry of all metal centers is C_3. The three-dimensional network is formed by the $[Cr(ox)_3]^{3-}$ complexes bridged by the Na^+ ions, and it provides perfect cavities for the size and the geometry of the $[M^{II}(bpy)_3]^{2+}$ complexes. The structure of the oxalate network is stabilized by the templating effect of the tris-bipyridine complexes through electrostatic interactions as well as π−π interactions between the oxalate and the bipyridine ligands. Table 1 reports structural parameters obtained from single crystals of the neat compounds, which will be relevant for the discussion of the spectroscopic properties. In addition to the lattice parameters, the unit cell volumes, Cr−O and Na−O bond lengths, and the interplane distances between oxalate ligands and the nearest and next-nearest neighbor bipyridine ligands are given.

X-ray powder diffraction patterns were recorded for the series of mixed crystals with composition $[Zn_{1-x}Ru_x(bpy)_3][NaCr(ox)_3]$ synthesized as described in section 2. Figure 1 shows an enlarged part of the diffraction patterns in the range of 17.9° ≤ 2θ ≤ 21.7°. The lattice

(7) Booth, H.S., G. M. *Inorg. Synth.* **1939**, *1*, 35.
(8) Palmer, R. A.; Piper, T. S. *Inorg. Chem.* **1966**, *5*, 864.
(9) *X-AREA*; Stoe & Cie GmbH, Darmstadt, Germany, 2005.
(10) Palatinus, L.; Chapuis, G. *J. Appl. Crystallogr.* **2007**, *40*, 786.
(11) Betteridge, P. W.; Carruthers, J. R.; Cooper, R. I.; Prout, K.; Watkin, D. J. *J. Appl. Crystallogr.* **2003**, *36*, 1487.
(12) Rodriguez-Caravajal, J. *Physica B* **1993**, *192*, 55.
(13) Sieber, R.; Decurtins, S.; Stoeckli-Evans, H.; Wilson, C.; Yufit, D.; Howard, J. A. K.; Capelli, S. C.; Hauser, A. *Chem.—Eur. J.* **2000**, *6*, 361.
(14) Shen, Y. R.; Holzapfel, W. B. *Phys. Rev. B* **1995**, *52*, 12618.

Table 1. Lattice Constant *a*, Average Cr−O Bond Lengths, Cr−M^{2+} Distance between a Given Cr^{3+} and the Seven M^{2+} Ions of the Nearest Neighbor Shell, and Interplane Distance between Oxalate Ligands and the Bipyridine Ligands of the Next and Next-Nearest Neighbors for $[Zn(bpy)_3][NaCr(ox)_3]$ and $[Ru(bpy)_3][NaCr(ox)_3]$ Single Crystals at Room Temperature

	a [Å]	Cr−O [Å]	Na−O [Å]	Cr−M^{2+} (1st) [Å]	Cr−M^{2+} (2nd) [Å]	Cr−M^{2+} (3rd) [Å]	π(bpy)−π(ox) (1st) [Å]	π(bpy)−π(ox) (2nd) [Å]
$[Zn(bpy)_3][NaCr(ox)_3]$	15.6365(18)	1.9695(2)	2.371(3)	6.1712(7)	8.586(1)	9.236(1)	3.634	3.623
$[Ru(bpy)_3][NaCr(ox)_3]$	15.5098(6)	1.9685(3)	2.339(3)	6.1501(8)	8.5150(9)	9.1453(9)	3.755	3.730

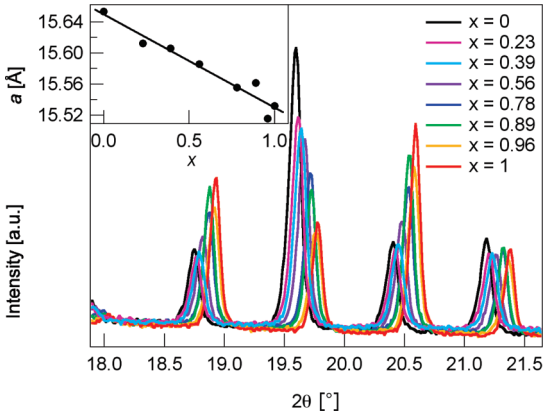

Figure 1. Powder diffraction patterns of $[Zn_{1-x}Ru_x(bpy)_3][NaCr(ox)_3]$, with $x = 0$, 0.23, 0.39, 0.56, 0.78, 0.89, 0.96, and 1 at room temperature. The inset shows the evolution of the lattice parameter *a* as a function of the mole fraction *x* of $[Ru(bpy)_3]^{2+}$ as obtained from profile matching using the FullProf software.[12]

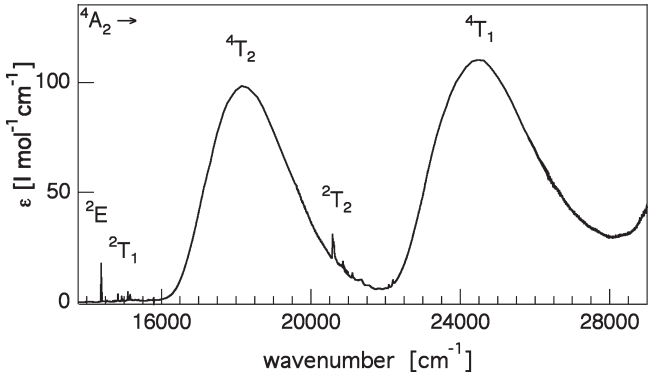

Figure 2. Single crystal absorption spectrum of $[Zn(bpy)_3][NaCr(ox)_3]$ at 10 K and 2.0 cm^{-1} spectral resolution.

parameter *a* was obtained by profile matching after entering the space group, the fractional coordinates of all atoms for the neat $[Zn(bpy)][NaCr(ox)_3]$ from the literature,[13] and the approximate lattice parameter *a* as a starting value. *a* is shown as a function of the effective $[Ru(bpy)_3]^{2+}$ mole fraction *x* as determined by ICP-MS in the inset of Figure 1. It decreases linearly with increasing $[Ru(bpy)_3]^{2+}$ mole fraction, going from 15.6531 Å to 15.5318 Å for *x* from 0 to 1, thus obeying Vegard's law.[15] The corresponding unit cell volume decreases from 3835.3 to 3746.8 $Å^3$, that is, by 92.2 $Å^3$ or 2.4%. The small apparent difference between the lattice parameters obtained from powder and single crystals of the same compound is probably due to a small shift of the origin for the former. Thus, the difference is not related to the structure of the oxalate network, and for the discussion, the lattice parameters obtained from the single crystal determinations will be used.

3.2. Electronic Absorption Spectroscopy. Figure 2 shows the single crystal absorption spectrum of $[Zn(bpy)_3][NaCr(ox)_3]$ from 14 000 to 29 000 cm^{-1}. In accordance with previously published spectra of compounds with $[Cr(ox)_3]^{3-}$ as a chromophore,[16−18] the broad bands centered at 17 889 cm^{-1} and 24 270 cm^{-1} are readily attributed to the spin-allowed $^4A_2 \rightarrow {}^4T_2$ and $^4A_2 \rightarrow {}^4T_1$ transitions, respectively. The weak and sharp features at 14 400, 14 800, and 20 580 cm^{-1} are assigned to the spin-flip transitions $^4A_2 \rightarrow {}^2E$, $^4A_2 \rightarrow {}^2T_1$, and $^4A_2 \rightarrow {}^2T_2$, respectively. Ligand field parameters can be estimated using the energies of $^4A_2 \rightarrow {}^4T_2$, $^4A_2 \rightarrow {}^4T_1$, and $^4A_2 \rightarrow {}^2E$ transitions and the Tanabe and Sugano energy matrices.[19] Hence, the ligand field parameters are 10Dq ≈ 17 889 cm^{-1}, $B \approx 617\ cm^{-1}$, and $C \approx 3249\ cm^{-1}$. Those parameters are close to the ones obtained for ruby,[20,21] 10Dq ≈ 18 100 cm^{-1}, $B \approx 650\ cm^{-1}$, and $C \approx 3200\ cm^{-1}$.

As mentioned above, the lowest energy transition of Cr^{3+} in $[Cr(ox)_3]^{3-}$ in a strong ligand field is the spin-forbidden $^4A_2 \rightarrow {}^2E$ spin-flip transition of a d^3 ion. At 10 K, it appears as two sharp zero-phonon lines (R-lines) with relatively small inhomogeneous line widths and relatively large extinction coefficients. These characteristics make it ideal for studying the structural homogeneity around the Cr^{3+} ions. A minor change in the local environment can be followed by the evolution of the $^4A_2 \rightarrow {}^2E$ band shape. Consequently, local structural information on $[Zn_{1-x}Ru_x(bpy)_3][NaCr(ox)_3]$ mixed crystals can be obtained by analyzing the $^4A_2 \rightarrow {}^2E$ transition as a function of *x*. Figure 3 shows the single crystal absorption spectra at 0.5 cm^{-1} spectral resolution in the region of the R-lines for $x = 0$, 0.18, 0.31, 0.44, 0.58, 0.76, 0.90, and 1. The spectrum of the neat compound $[Zn(bpy)_3][NaCr(ox)_3]$ consists of two Gaussian bands corresponding to the R_1 and R_2 lines. A zero-field splitting (ZFS) of the ^2E level of 15.2 cm^{-1} and an inhomogeneous line width of 2.1 cm^{-1} is obtained from a least-squares fit to a Gaussian profile. This is in accordance with values observed for $[Cr(ox)_3]^{3-}$ in other hosts and matrices.[6,16,22] The ZFS of the $^4A_2$ ground state is not resolved. The origin of the ZFS of the $^4A_2$ and ^2E levels is the trigonal distortion (C_3 site symmetry[13]) and the spin−orbit coupling of the d^3 ion. For $[Ru(bpy)_3][NaCr(ox)_3]$, the inhomogeneous line width is somewhat smaller, and the ZFS of the $^4A_2$ ground state is resolved in the absorption spectrum of both R lines. Fitting each R-line

(15) Vegard, L. *Z. Phys.* **1921**, *5*, 17.
(16) Schönherr, T.; Spanier, J.; Schmidtke, H. H. *J. Phys. Chem.* **1989**, *93*, 5969.
(17) Milos, M.; Kairouani, S.; Rabaste, S.; Hauser, A. *Coord. Chem. Rev.* **2008**, *252*, 2540.
(18) Piper, T. S.; Carlin, R. L. *J. Chem. Phys.* **1961**, *35*, 1809.
(19) Tanabe, Y.; Sugano, S. *J. Phys. Soc. Jpn.* **1954**, *9*, 753.
(20) Munro, R. G. *J. Chem. Phys.* **1977**, *67*, 3146.
(21) Tanabe, Y.; Sugano, S. *J. Phys. Soc. Jpn.* **1956**, *11*, 864.
(22) Riesen, H. *Coord. Chem. Rev.* **2006**, *250*, 1737.

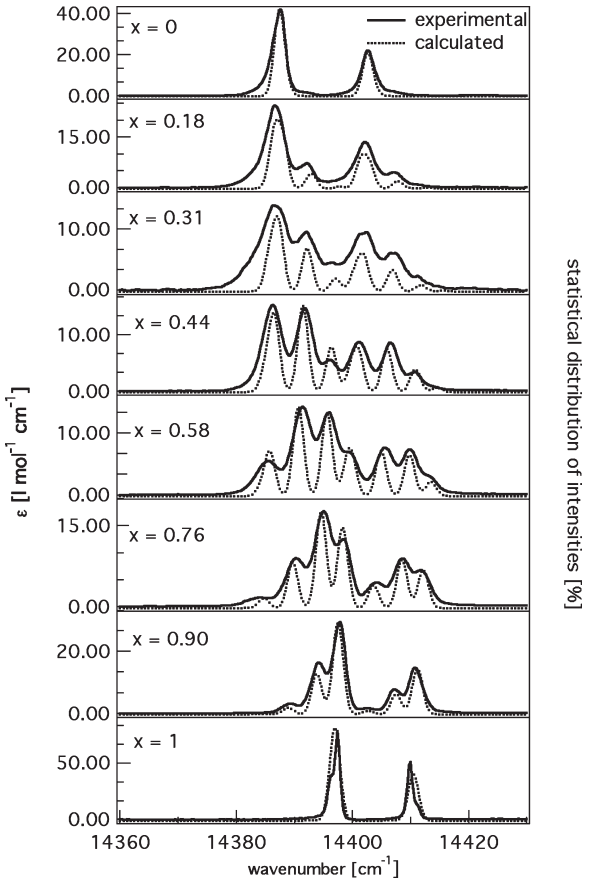

Figure 3. Single crystal absorption spectra of $[Zn_{1-x}Ru_x(bpy)_3][NaCr(ox)_3]$ at 10 K in the region of the $^4A_2 \rightarrow {}^2E$ transition, (—) experimental, (···) simulated as described in the text.

with two Gaussians results in an inhomogeneous line width of 1.1 cm^{-1} and a ZFS of the $^4A_2$ ground state of 1.3 cm^{-1}, which is likewise in the range observed for this compound.[16,17,22] As compared to the neat $[Zn(bpy)_3]^{2+}$ compound, the ZFS of the ^2E state has decreased to 12.5 cm^{-1}, and the R-lines appear shifted to higher energies by ~10 cm^{-1}.

The absorption spectra of the mixed crystals do not at all show the initially expected smooth transition from the spectrum of one of the neat compounds to the spectrum of the other one, with at most an increase in the inhomogeneous line width for a certain range of x. Instead, they show additional and distinct splittings of the R lines. These splittings and the relative intensities of the resulting multiline spectrum can be quantitatively modeled (for a discussion see section 4) on the basis of five distinct spectroscopic sites, which appear with different concentrations as a function of the Ru^{2+} mole fraction across the series. On the basis of this observation, the ZFS of the ^2E state can be simply obtained by taking the energy difference between corresponding R lines. The analysis reveals that the ZFS of the ^2E state is within experimental accuracy independent of the specific site and only depends on the given Ru^{2+} mole fraction.

3.3. High-Pressure Luminescence Experiments. Figure 4a and b show the luminescence of the R lines of $[Ru(bpy)_3][NaCr(ox)_3]$ and $[Zn(bpy)_3][NaCr(ox)_3]$, respectively, at different pressures going from 0 to 1.2 GPa and at 10 K. Even in the neat compounds, the luminescence of the spin-flip transitions shifts to lower energies by about 1.5 cm^{-1} as compared to the absorption because of efficient energy migration within the ^2E state.[23] The insets of Figure 4a and b show the shift of the R_1 line as a function of external pressure as determined from Gaussian fits to the emission bands. The shift is linear and within experimental error identical for both compounds for pressures up to 1 GPa. This is not surprising as the compressibilities of the two compounds are expected to be very similar. The shift rate of -25.2 ± 1.2 cm^{-1}/GPa itself, however, is more than three times greater than the shift rate of the R_1 line of Cr^{3+} in ruby, the latter being -7.59 cm^{-1}/GPa.[23] It is due to the higher compressibility of the three-dimensional oxalate network compounds compared to ruby. As will be discussed in more detail in section 4, in the softer material, there is a more pronounced increase of the nephelauxetic effect with applied pressure, for which both a shortening of the Cr−O bond lengths and an increase in $\pi-\pi$ interactions between oxalate and bipyridine ligands are responsible. Above ~1 GPa, a doubling of the R-lines in $[Zn(bpy)_3][NaCr(ox)_3]$ indicates a pressure-induced crystallographic phase transition.

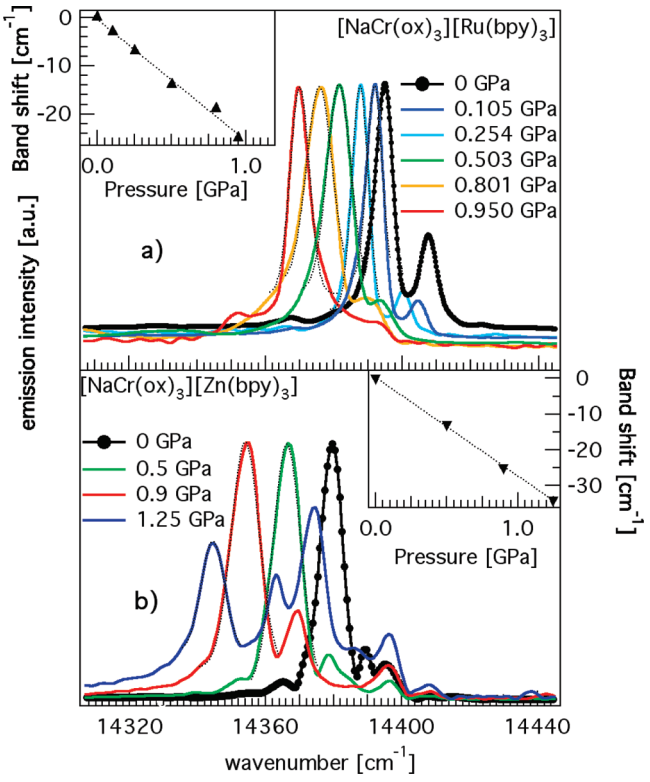

Figure 4. (a) Luminescence spectra of $[Ru(bpy)_3][NaCr(ox)_3]$ (●) under atmospheric pressure at 15 K and under different external pressures up to 1 GPa (—) at 10 K. The inset shows the dependence of the R_1 line with external pressure. (b) Luminescence spectra of $[Zn(bpy)_3][NaCr(ox)_3]$ at 10 K under atmospheric pressure (●) and after applying different external pressures. The inset shows the dependence of the R_1 band shift with pressure.

4. Discussion

4.1. Absorption Spectroscopy and Specific Spectroscopic Sites. Within the three-dimensional network, the chromium oxalates are bridged by sodium ions making

(23) Bray, K. L. *Top. Curr. Chem.* **2001**, *213*, 1.

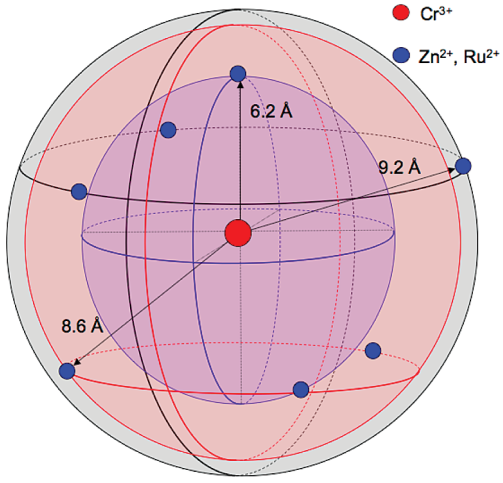

Figure 5. Schematic representation of the nearest-neighbor shell around a given Cr^{3+} ion.

cavities in which the tris-bipyridine complexes are embedded. The three-dimensional structure can be simplified by considering a given Cr^{3+} ion and the neighboring M^{2+} ions. As schematically shown in Figure 5, the closest M^{2+} ion sits on the 3-fold axis of the central ion at a distance of 6.2 Å. Three other M^{2+} ions are found at a distance of 8.6 Å, and the next three at 9.2 Å. These seven M^{2+} ions make up the nearest neighbor shell around a given Cr^{3+} ion. The closest M^{2+} neighbor to the Cr^{3+} has all three bipyridine ligands interacting with each oxalate ligand of the Cr^{3+} via a very good $\pi-\pi$ overlap. The next three M^{2+} ions, sitting at 8.6 Å, have one of their three bipyridines that have an optimal overlap with one of the oxalates of the Cr^{3+}. The other two bipyridine ligands interact with the next Cr^{3+} ions in the lattice. For the last three, the $\pi-\pi$ interactions between oxalate and bipyridine ligands are weak since the ligand planes are orthogonal to each other.[24,25] The origin of the 5 specific experimentally observed spectroscopic sites in the mixed crystal series $[Zn_{1-x}Ru_x(bpy)_3][NaCr(ox)_3]$ can thus be explained by considering the distribution of Zn^{2+} and Ru^{2+} among the four nearest $[M(bpy)_3]^{2+}$ neighbors of a given $[Cr(ox)_3]^{3-}$ complex for which non-negligible $\pi-\pi$ interactions occur. A given Cr^{3+} ion can be surrounded by four Zn^{2+} ions. Such a site will be labeled (4,0). A Cr^{3+} surrounded by three Zn^{2+} and one Ru^{2+} ion will be labeled (3,1). Accordingly, the three other sites are labeled (2,2) and (1,3) for two or one Zn^{2+} and two or three Ru^{2+} ions, respectively, and (0,4) when all four positions are occupied by Ru^{2+}. Sites (3,1), (2,2), and (1,3) each have two subsites with different weights due to the fact that the four nearest M^{2+} neighbors are not at the same distance from the central ion, one being 2.3 Å closer than the other three. In Figure 3, the subsites are not resolved spectroscopically and will thus be neglected in the following. However, it is possible that they give rise to a somewhat larger inhomogeneous broadening of the corresponding absorption bands.

(24) Langford, V. S.; von Arx, M. E.; Hauser, A. *J. Phys. Chem. A* **1999**, *103*, 7161.
(25) Hauser, A.; von Arx, M. E.; Langford, V. S.; Oetliker, U.; Kairouani, S.; Pillonnet, A. *Top. Curr. Chem.* **2004**, *241*, 65.

The population of the 5 spectroscopic sites depends on the relative concentrations of Ru^{2+} and Zn^{2+}. For $x = 0$ and 1, only sites (4,0) and (0,4), respectively, are populated. For arbitrary values of x, the population of site $(N-n, n)$ is given by a binomial distribution

$$p_n(x) = \binom{N}{n} \cdot (1-x)^{N-n} \cdot x^n \quad N = 4, \text{ and } n = 0, 1, 2, 3, 4 \tag{1}$$

The exact energy of the R-lines is modeled to depend upon x taking into account the global variation of the lattice constant, on the one hand, and upon the specific environment according to the binomial distribution, on the other hand. For the former, we expect a linear red shift with an increasing value of x due to the fact that, for the neat Ru compound, the lattice parameter a is smaller than for the neat Zn compound, which directly results in a reduction of the average Cr−O bond length, which, in turn, results in a reduction of the electronic repulsion due to an increasing electronic delocalization toward the ligands (nephelauxetic effect).[26,27] The latter results in a stepwise shift to higher energies with an increasing number of Ru^{2+} ions in the nearest neighbor shell. This is due to the decreasing $\pi-\pi$ interaction between oxalate and bipyridines and thus a decreasing nephelauxetic effect, because replacing Zn^{2+} with Ru^{2+} results in an increasing distance between bipyridine and oxalate ligand planes (see Table 1). Thus, the positions of the R_1 and R_2 lines for each of the five sites as a function of x may be described by

$$\tilde{\nu}_{ni}(x) = \tilde{\nu}^0_{ni} - b_i x \quad i = 1, 2 \tag{2}$$

where $\tilde{\nu}^0_{ni}$ are the positions of R-lines of the site with n nearest neighbor Ru^{2+} ions extrapolated to $x = 0$ and b takes into account the global effect of an increasing Ru^{2+} concentration. With relative oscillator strengths of the R-lines to be $f_1/f_2 = 2{:}1$ taken directly from the spectrum at $x = 0$, and neglecting the variation in the inhomogeneous bandwidth by assuming an average value of 2 cm^{-1} full width at half-maximum, the absorption spectrum is given by a sum of Gaussians for each R-line according to

$$A_i(\tilde{\nu}) \sim f_i \sum_n \left(\binom{N}{n} \cdot (1-x)^{N-n} \cdot x^n \right) \cdot \exp\left(-\frac{(\tilde{\nu} - (\tilde{\nu}^0_{ni} - b_i x))^2}{2\sigma^2} \right) \quad i = 1, 2 \tag{3}$$

There are 4 fitting parameters in eq 3, namely, $\tilde{\nu}^0_{1,1}$, $\tilde{\nu}^0_{2,1}$, $\tilde{\nu}^0_{3,1}$, and b_1. The other constants such as $\tilde{\nu}^0_{0,1}$, $\tilde{\nu}^0_{4,1}$, all the $\tilde{\nu}^0_{n,2}$ of the R_2 line, and b_2 can either be obtained directly from the experiment at $x = 0$ and 1 or be expressed as functions of the first four fitting parameters. Thus, $\tilde{\nu}^0_{4,1} = \tilde{\nu}^1_{4,1} + b_1$, $\tilde{\nu}^0_{n,2} = \tilde{\nu}^0_{n,1} + D(^2E)^0_4$, where $D(^2E)^0_4$ is the ZFS of the ^2E state of the site (4,0) for $x = 0$, and $b_2 = \tilde{\nu}^1_{4,1} - \tilde{\nu}^1_{4,2} + D(^2E)^0_4 + b_1$, where the superscript

(26) Schäffer, C. E.; Jørgensen, C. K. *J. Inorg. Nucl. Chem.* **1958**, *8*, 143.
(27) Jørgensen, C. K. *Discuss. Farad. Soc* **1958**, 110.

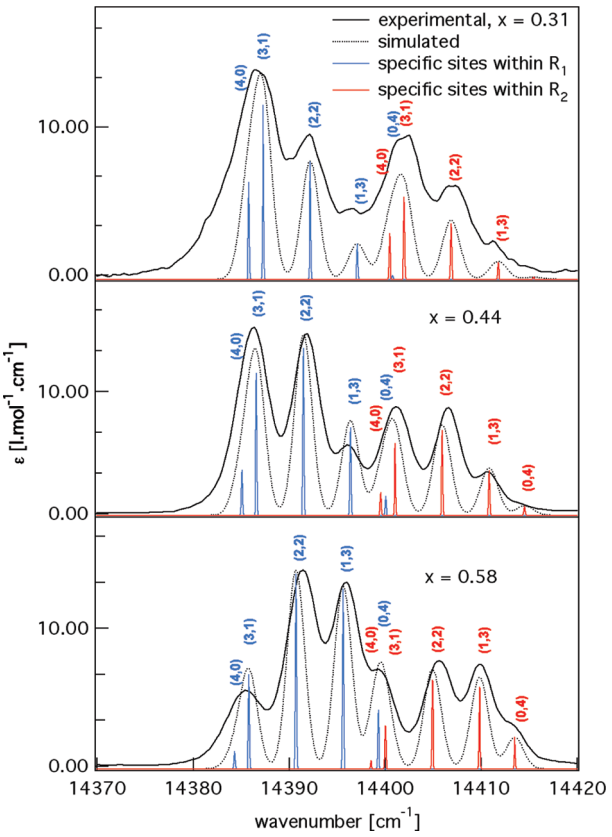

Figure 6. The energies of the individual sites for Ru^{2+} mole fraction x = 0.31, 0.44, and 0.58 in the mixed crystal series $[Zn_{1-x}Ru_x(bpy)_3][NaCr(ox)_3]$ at 10 K.

refers to $x = 1$. The simultaneous best fit of eq 3 to all the experimental spectra of Figure 3 gives initial positions at 14 387.5, 14 389.0, 14 393.9, 14 398.8, and 14 402.5 cm^{-1} for the R_1-line of the sites (4,0), (3,1), (2,2), (1,3), and (0,4), respectively, and $b_1 = 5.5$ cm^{-1}, and 14 402.7, 14 404.2, 14 409.1, 14 414.0, and 14 417.7 cm^{-1} for the R_2-line and $b_2 = 7.2$ cm^{-1}. Figure 3 includes the calculated absorption spectra using the above parameters. The overall agreement between experimental and calculated spectra across the series is good. The biggest deviations are due the variation in the inhomogeneous broadening, which is larger for the distributions with high concentrations of subsites which are not resolved spectroscopically.

In order to further illustrate this, Figure 6 indicates the positions of the five individual sites for three different compositions. The model developed in this paper shows clearly that several sites are hidden within the same band. For example, the band at 14 399 cm^{-1} of the compound with $x = 0.58$ is composed of three sites, $R_1(0,4)$, $R_2(3,1)$, and $R_2(4,0)$. This is the principle reason why it is difficult to extract the ZFS of individual sites for the different concentrations directly from the experimental data. In this multisite system, neither FLN nor hole burning spectroscopy on the individual sites are possible, the former due to efficient excitation energy transfer[16] and the latter due to the fact that, in the very well crystallized three-dimensional oxalate network, persistent hole burning is not observed.

4.2. Chemical and Physical Pressure on $[Cr(ox)_3]^{3-}$. The basic effect of pressure on any molecular solid is to decrease its volume. As a result, not only structural parameters such as bond angles and bond lengths but also intra- and intermolecular interactions change, thus affecting chemical, electrical, optical, and magnetic properties of the material. With regard to optical properties, absorption and emission bands shift with pressure either to higher or lower energies depending upon the nature of the states involved. Materials with high bulk moduli are more difficult to compress, and thus exhibit small volume changes per unit pressure and generally show smaller pressure shifts of electronic states in comparison to systems with low bulk moduli. An example of a hard material is ruby with a bulk modulus of 253 GPa[28,29] and a shift of -7.59 cm^{-1}/GPa, that is, to lower energies,[30] for the $^4A_2 \rightarrow {}^2E$ transition. The isothermal compressibility κ is the inverse of the bulk modulus K and gives an indication of the sensitivity of a system to pressure:[31,32,33]

$$\kappa = -\frac{1}{V}\left(\frac{\partial V}{\partial P}\right)_T = \frac{1}{K} \qquad (4)$$

Brillouin scattering experiments on the related system $[Rh(bpy)_3][NaCr(ox)_3]ClO_4$ gave a value for K of ~10 GPa.

When applying pressure on $[M^{II}(bpy)_3][NaCr(ox)_3]$, two important geometrical parameters are influenced: the Cr−O bond length decreases and the interplane separation between oxalate and bipyridine ligands decreases likewise. Both effects contribute to the observed red shift. When the Cr−O bond length decreases, the Racah parameters B and C decrease as well because of increased delocalization of electrons onto the oxalate ligands. When the interplane separation between the oxalates and the bipyridines decreases, $\pi-\pi$ interactions increase, leading to a further delocalization of electron density from the oxalate ligands to the bipyridines and amplifying the nephelauxetic effect. With -25.2 cm^{-1} GPa^{-1}, the resulting shift rate of the $^4A_2 \rightarrow {}^2E$ transition is thus quite large compared to ruby[23] and other Cr^{3+} doped lattices.[34−36]

The lattice parameters a as obtained for $[Zn(bpy)_3][NaCr(ox)_3]$ and $[Ru(bpy)_3][NaCr(ox)_3]$ from X-ray diffraction are 15.6365 Å and 15.5098 Å, respectively. Thus, replacing Zn^{2+} with Ru^{2+} decreases the unit cell volume by 92.2 $Å^3$ or 2.4%. For a bulk modulus of 10 GPa, the same decrease in volume requires an external pressure of ~0.24 GPa. Thus, for an external pressure of 0.24 GPa, which reduces the volume of $[Zn(bpy)_3][NaCr(ox)_3]$ to that of $[Ru(bpy)_3][NaCr(ox)_3]$ at ambient pressure, the R_1-line shifts by approximately 6.0 cm^{-1} to lower energy. This value has to be compared to the b_i ($i = 1, 2$) parameters of the model described in section 4.1. It is indeed very close to the average value of 6.5 cm^{-1} obtained from the fit for the latter. Hence, the b_i parameters

(28) Jephcoat, A. P.; Hemley, R. J.; Mao, H. K.; Cohen, R. E.; Mehl, M. J. *Phys. Rev. B* **1988**, *37*, 4727.
(29) Richet, P.; Xu, J. A.; Mao, H. K. *Phys. Chem. Miner.* **1988**, *16*, 207.
(30) Piermarini, G. J.; Block, S.; Barnett, J. D.; Forman, R. A. *J. Appl. Phys.* **1975**, *46*, 2774.
(31) Kittel, C., *Introduction to Solid State Physics*; John Wiley & Sons: New York, 2005.
(32) Cohen, M. L. *Phys. Rev. B* **1985**, *32*, 7988.
(33) Ecolivet, C.; Rabaste, S. Unpublished results.
(34) Shen, Y. R.; Riedener, T.; Bray, K. L. *Phys. Rev. B* **2000**, *61*, 11460.
(35) Wamsley, P. R.; Bray, K. L. *J. Lumin.* **1995**, *63*, 31.
(36) Grinberg, M.; Suchocki, A. *J. Lumin.* **2007**, *125*, 97.

have a physical significance and correspond to the energy shift of the luminescence band solely due to the volume contraction on going from $[Zn(bpy)_3][NaCr(ox)_3]$ to $[Ru(bpy)_3][NaCr(ox)_3]$ while keeping the immediate chemical environment of a given site unchanged.

The crystallographic data given in Table 1 show that, when replacing $[Zn(bpy)_3]^{2+}$ with $[Ru(bpy)_3]^{2+}$, the Cr−O distance decreases only very slightly but statistically significantly by 0.001 Å, that is, from 1.970 Å to 1.969 Å, while the distance between the oxalate and bipyridine planes increases more strongly, that is, from 3.634 Å to 3.755 Å for the nearest-neighbor pair. As for external pressure, the Cr−O bond length decreases upon reduction of the unit cell parameter, but in contrast to external pressure, the substitution of Zn^{2+} by the smaller Ru^{2+} results in a reduced $\pi-\pi$ interaction. Thus, in contrast to external pressure, the relevant geometric changes upon substitution work in opposite directions. With regard to the oxalate network, the reduction in the size of the $[M(bpy)_3]^{2+}$ ion is absorbed by the Na−O bond rather than by the Cr−O bond, and therefore overall, the effect of the change in $\pi-\pi$ interaction dominates. Thus, for the neat compounds, $[Zn(bpy)_3][NaCr(ox)_3]$ and $[Ru(bpy)_3][NaCr(ox)_3]$ with only one specific site, (4,0) and (0,4), respectively, the R-lines shift to higher energies by $\sim$10 cm^{-1} despite the decrease in Cr−O bond length. Within the mixed crystal series, the decrease of the $\pi-\pi$ interaction strength when substituting the Zn^{2+} with Ru^{2+} sequentially around a given Cr^{3+} is responsible for the discrete shifts to higher energies, while the small decrease of the Cr−O bond length with increasing $[Ru(bpy)_3]^{2+}$ mole fraction is responsible for the small shift to lower energies of each individual specific site. For comparison, in ruby, a reduction of the Cr−O bond length of 0.001 Å requiring an external pressure of $\sim$0.5 GPa results in a red shift of the same order of magnitude.

5. Conclusions

In the series of mixed crystals with composition $[Zn_{1-x}Ru_x(bpy)_3][NaCr(ox)_3]$, distinct sites are created for each Cr^{3+} ion. High-resolution absorption spectroscopy, high-pressure luminescence experiments, and crystallographic data allowed some clear-cut conclusions about the relation between the geometric and electronic structure of Cr^{3+} in the three-dimensional oxalate network lattices. The specific sites arise according to the distribution of the four closest M^{2+} positions around the Cr^{3+}. Thus, five specific sites are resolved spectroscopically. Each individual site shifts to lower energy when the mole fraction of $[Ru(bpy)_3]^{2+}$ is increased. This is due to the shortening of the Cr−O bond length, and thus decreasing Racah parameters. On the other hand, the energies of each specific site increase with an increasing number of $[Ru(bpy)_3]^{2+}$ on the four specific positions around a given Cr^{3+}. This is due to the decrease of the $\pi-\pi$ interaction when a smaller $[M(bpy)_3]^{2+}$ complex is sitting in the oxalate cavity. Thus, the nephelauxetic effect decreases and the R_1 and R_2 of each site discretely shift to higher energies. In this paper, we developed a simple model that nicely fits the absorption spectra of the mixed crystal series. The population of each site was modeled with a statistical binomial distribution, while the energy of the ^2E transition of each site and its dependence on the $[Ru(bpy)_3]^{2+}$ mole fraction was modeled with reference to high-pressure experiments on the neat $[Ru(bpy)_3][NaCr(ox)_3]$ compound. With our results, we demonstrate the importance of $\pi-\pi$ interactions in the second coordination shell even for the photophysical properties of involved metal-centered d−d transitions.

Acknowledgment. The authors thank the Swiss National Science Foundation (grant number 200020-125175) for funding, C. Besnard for the crystal structure of the ruthenium compound, F. Kubel for advice regarding the evaluation of the powder diffraction data, N. Amstutz for her help in the preperation of the samples, and H. Hagemann for his help with the pressure experiments.

Supporting Information Available: Crystallographic details for $[Ru(bpy)_3][NaCr(ox)_3]$ (CIF file). This material is available free of charge via the Internet at http://pubs.acs.org.